

Hydrogen and Helium Burning in Type I X-ray Bursts: Experimental Results and Future Prospects

Catherine M. Deibel
Louisiana State University

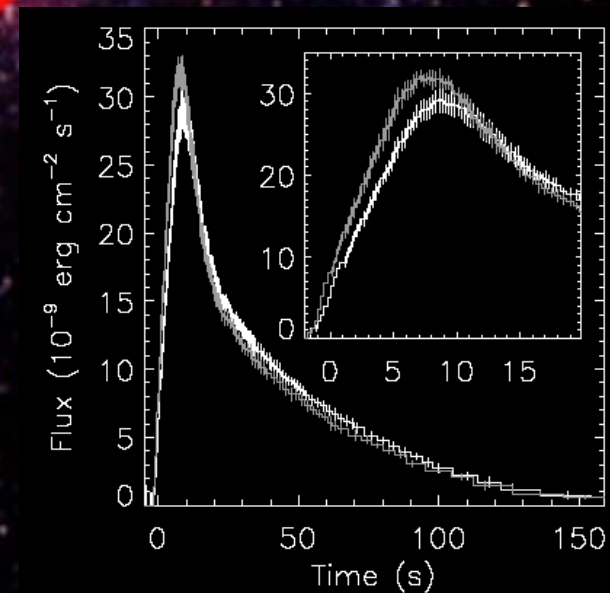
Type I X-Ray Bursts (XRBs)

Neutron stars:
 $1.4 M_{\odot}$, 10 km radius

Normal star

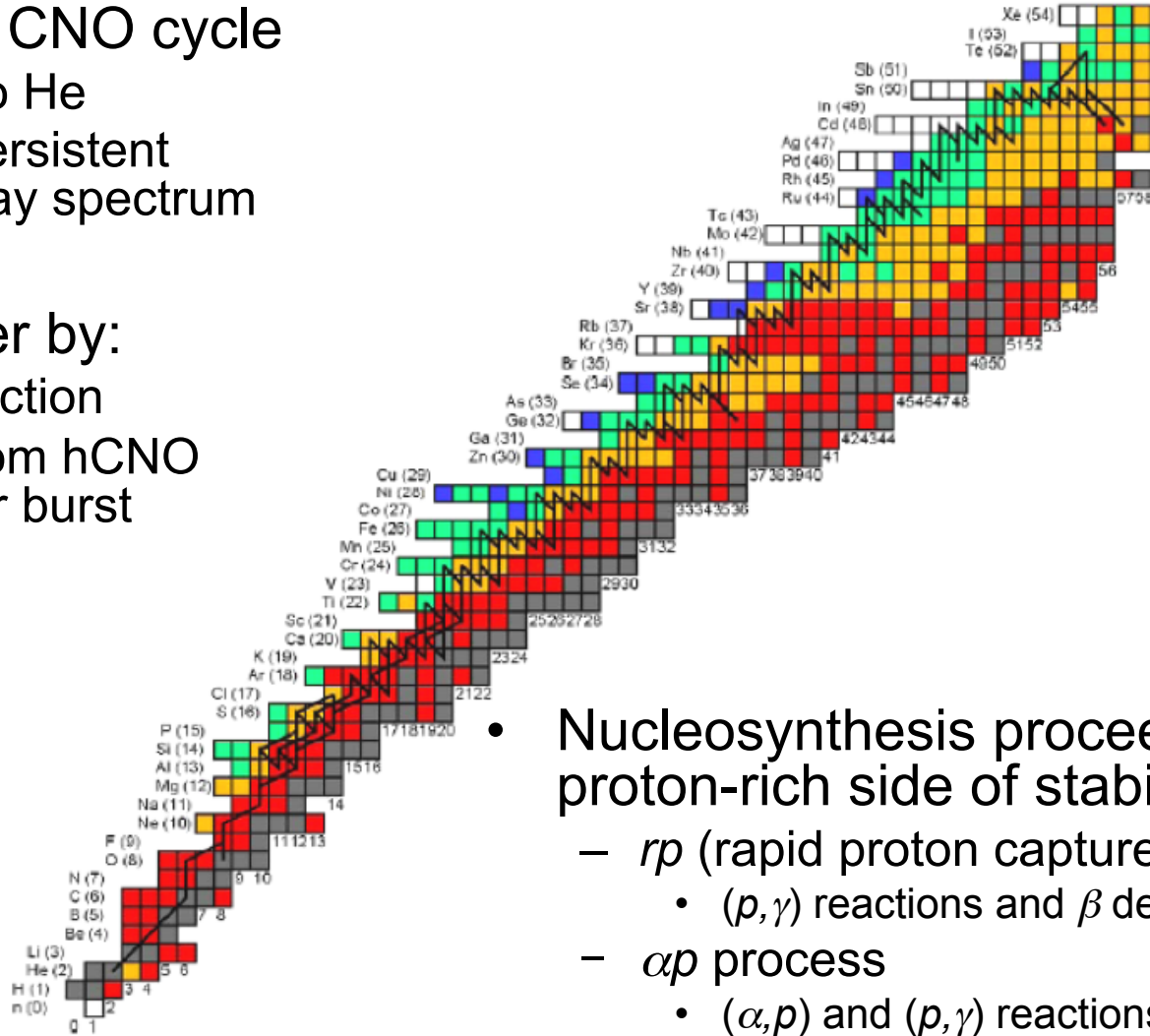


Accretion rate $\sim 10^{-8}/10^{-10} M_{\odot}/\text{year}$
Peak x-ray burst temperature $\sim 1.5 \text{ GK}$
Recurrence rate $\sim \text{hours to days}$
Burst duration of 10 – 100 s
Observed x-ray outburst $\sim 10^{39} - 10^{40} \text{ ergs}$



X-Ray Burst Nucleosynthesis

- Pre-burst hot CNO cycle
 - burns H into He
 - results in persistent thermal X-ray spectrum
- Burst is trigger by:
 - Triple- α reaction
 - breakout from hCNO cycle trigger burst
 - $T \sim 10^8$ K

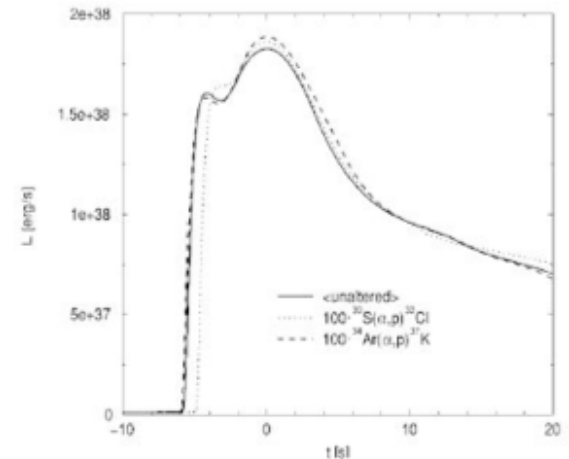


- Nucleosynthesis proceeds up proton-rich side of stability:
 - rp (rapid proton capture) process
 - (p, γ) reactions and β decays
 - αp process
 - (α, p) and (p, γ) reactions
 - peak temperatures of 1 – 2 GK

H. Schatz, K. E. Rehm, NPA **777**, 601 (2006)

Modeling XRBs

- Reaction rates are crucial
 - determine flow of burst
 - effect energy output
 - influence final elemental abundances
- Theoretical rates used in models for almost all reactions
 - based on Hauser-Feshbach theory
 - level densities may be low for many resonant reactions
- Not all reactions are created equally!
 - thousands of reactions involving radioactive nuclei . . . where to focus efforts?
 - sensitivity studies give some direction, but may not be the full story



J.L. Fisker, *et al.*, ApJ (2004).

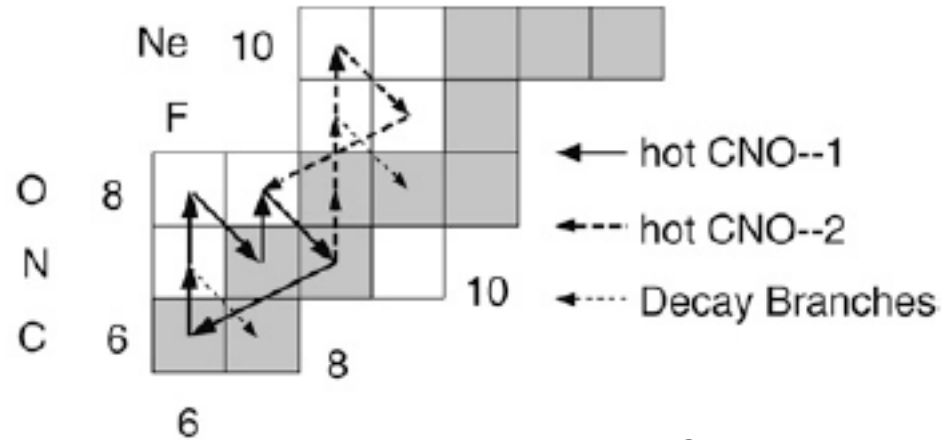
Table 19. Summary of the most influential nuclear processes, as collected from Tables 1–10. These reactions affect the yields of, at least, 3 isotopes when their nominal rates are varied by a factor of 10 up and/or down. See text for details.

Reaction	Models affected
$^{12}\text{C}(\alpha, \gamma)^{16}\text{O}^a$	F08, K04-B2, K04-B4, K04-B5
$^{16}\text{O}(\alpha, p)^{19}\text{F}^a$	K04-B1 ^b
$^{28}\text{Si}(\alpha, p)^{31}\text{P}$	K04-B5
$^{28}\text{Si}(\alpha, p)^{29}\text{Si}$	F08
$^{30}\text{Si}(\alpha, p)^{31}\text{P}$	K04-B5
$^{30}\text{P}(\alpha, p)^{31}\text{S}$	K04-B4
$^{32}\text{S}(\alpha, p)^{33}\text{Cl}$	K04-B4 ^c , K04-B5 ^b
$^{33}\text{Cl}(p, \gamma)^{34}\text{Ar}$	K04-B1
$^{36}\text{S}(\alpha, \gamma)^{40}\text{Ar}$	K04-B2
$^{60}\text{Ni}(\alpha, p)^{63}\text{Cu}$	S01 ^b , K04-B5
$^{67}\text{Cu}(p, \gamma)^{68}\text{Zn}$	F08
$^{68}\text{Cu}(p, \gamma)^{69}\text{Zn}$	S01 ^b , K04-B5
$^{68}\text{Ga}(p, \gamma)^{69}\text{Ge}$	F08, K04-B1, K04-B2, K04-B5, K04-B6
$^{76}\text{As}(p, \gamma)^{77}\text{Se}$	K04 ^b , K04-B1, K04-B2 ^b , K04-B3 ^b , K04-B4, K04-B5, K04-B6
$^{78}\text{Br}(p, \gamma)^{79}\text{Kr}$	K04-B7
$^{78}\text{Rb}(p, \gamma)^{79}\text{Sr}$	K04-B2
$^{82}\text{Zr}(p, \gamma)^{83}\text{Nb}$	K04-B6
$^{84}\text{Zr}(p, \gamma)^{85}\text{Nb}$	K04-B2
$^{88}\text{Nb}(p, \gamma)^{89}\text{Mo}$	K04-B6
$^{92}\text{Mo}(p, \gamma)^{93}\text{Tc}$	F08
$^{92}\text{Mo}(p, \gamma)^{93}\text{Tc}$	F08, K04-B6
$^{97}\text{Mo}(p, \gamma)^{98}\text{Tc}$	K04-B6
$^{100}\text{Ru}(p, \gamma)^{101}\text{Rh}$	K04-B2, K04-B6
$^{100}\text{Rh}(p, \gamma)^{101}\text{Pd}$	K04-B2
$^{106}\text{Ag}(p, \gamma)^{107}\text{Cd}$	K04, K04-B2, K04-B3, K04-B7
$^{107}\text{In}(p, \gamma)^{108}\text{Sn}$	K04, K04-B3
$^{107}\text{In}(p, \gamma)^{108}\text{Sn}$	K04-B3, K04-B7
$^{108}\text{Sn}(\alpha, p)^{109}\text{Sb}$	S01 ^b

A. Parikh *et al.*, ApJ SS (2008)

hCNO Breakout

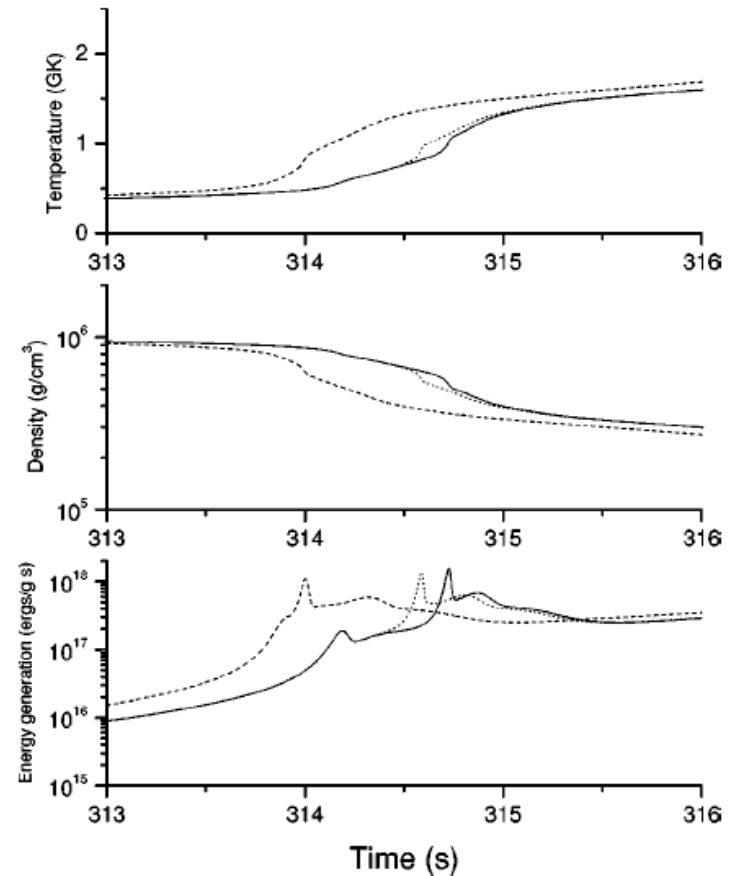
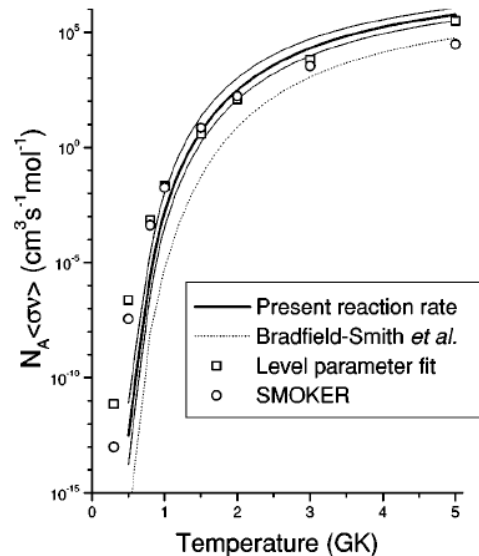
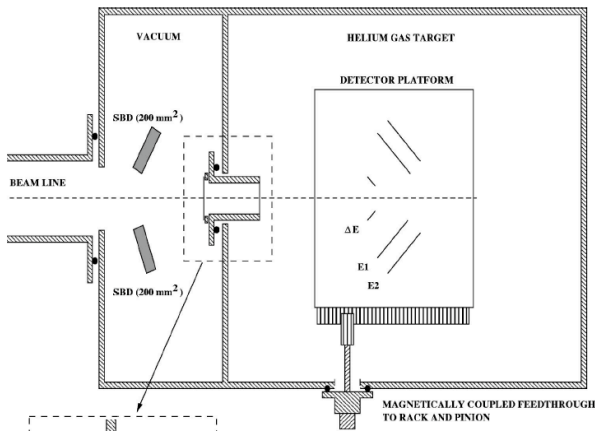
- Interplay between triple- α reaction and breakout from hCNO trigger burst
 - $^{15}\text{O}(\alpha, \gamma)^{19}\text{Ne}$
 - $^{18}\text{Ne}(\alpha, p)^{21}\text{Na}$
- Multiple direct and indirect measurements of $^{18}\text{Ne}(\alpha, p)^{21}\text{Na}$, but large discrepancies exist



M. Wiescher *et al.*, JPG **25**, R133 (1999)

Direct Study of $^{18}\text{Ne}(\alpha, p)^{21}\text{Na}$

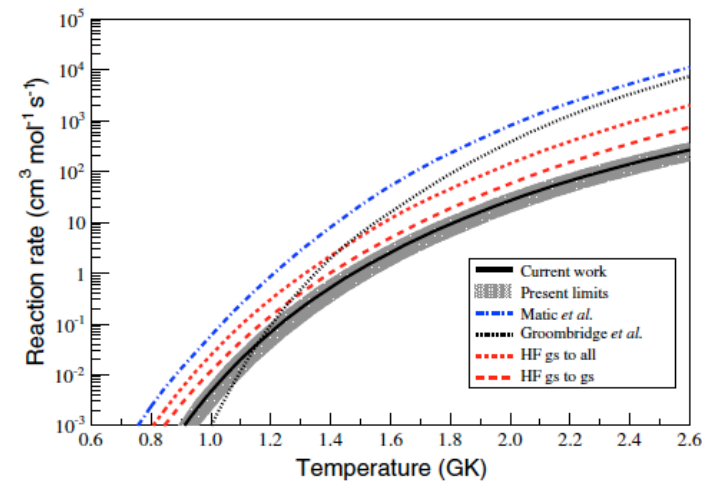
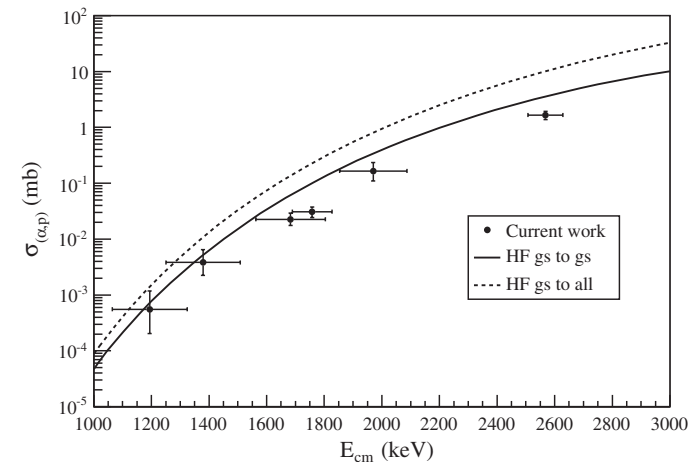
- Few direct measurements exist
 - lack of high intensity RIBs along path
 - difficulty with gas targets
- Direct $^{18}\text{Ne}(\alpha, p)^{21}\text{Na}$ reaction measurement at Louvain-la-Neuve between $E_{\text{cm}} = 1.7 - 2.6$ MeV
 - shows delay of hCNO breakout



Groombridge *et al.*, PRC **66**, 055802 (2002)

Indirect $^{18}\text{Ne}(\alpha, p)^{21}\text{Na}$ measurement

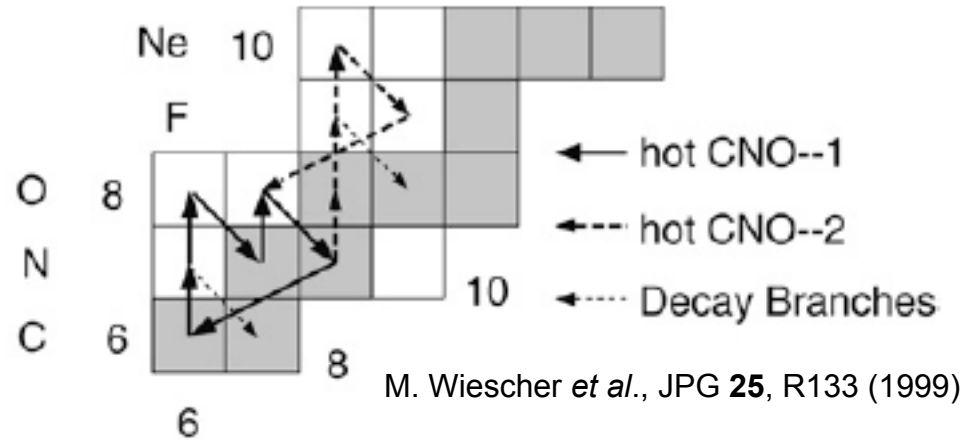
- Time inverse $^{21}\text{Na}(p, \alpha)^{18}\text{Ne}$ reaction performed at TRIUMF laboratory
 - ^{21}Na beam at six energies
 - CH_2 target
 - $E_{\text{cm}}(\alpha, p) = 1.17 - 2.57 \text{ MeV}$
- Results:
 - cross sections lower than theoretical calculations
 - lower rate leads to delay of breakout and higher temperatures at breakout point



P. J. C. Salter *et al*, PRL**108**, 242701 (2012)

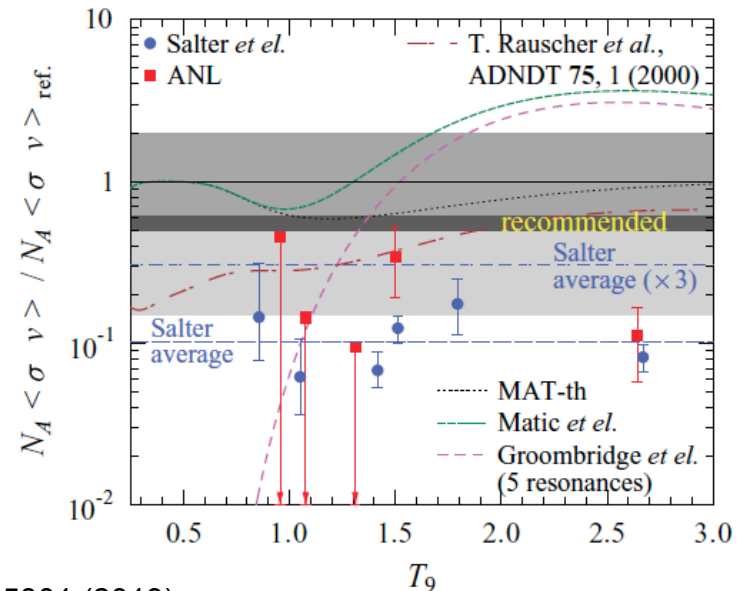
hCNO Breakout

- Interplay between triple- α reaction and breakout from hCNO trigger burst
 - $^{15}\text{O}(\alpha, \gamma)^{19}\text{Ne}$
 - $^{18}\text{Ne}(\alpha, p)^{21}\text{Na}$
- Multiple direct and indirect measurements of $^{18}\text{Ne}(\alpha, p)^{21}\text{Na}$, but large discrepancies exist



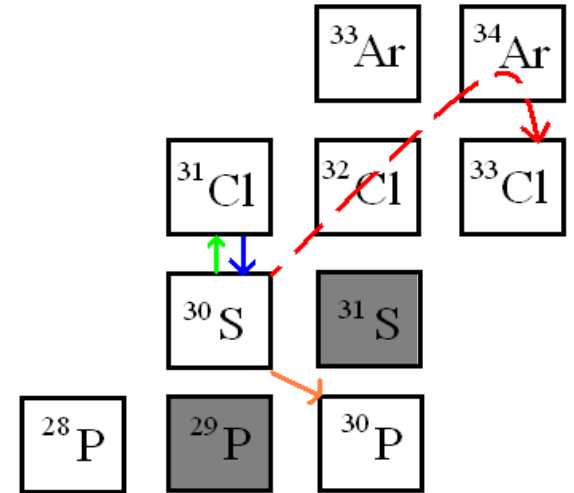
$E_{\text{eff}}(\alpha, p)$ (MeV)	Exponent for σ (mb)	σ_{exp}	Ref.	$\bar{\sigma}_{\text{ref.}}$	$\sigma_{\text{exp}}/\bar{\sigma}_{\text{ref.}}$
1.194 ± 0.130	10^{-4}	$5.5^{+6.2}_{-3.5}$	SAL	37.8	$0.145^{+0.164}_{-0.067}$
1.379 ± 0.129	10^{-3}	$3.8^{+2.7}_{-1.6}$	SAL	61.6	$0.062^{+0.044}_{-0.026}$
1.683 ± 0.121	10^{-2}	$2.3^{+0.7}_{-0.5}$	SAL	33.7	$0.068^{+0.021}_{-0.015}$
1.758 ± 0.069	10^{-2}	3.1 ± 0.6	SAL	25.1	0.124 ± 0.024
1.970 ± 0.117	10^{-1}	$1.7^{+0.7}_{-0.6}$	SAL	9.7	$0.175^{+0.073}_{-0.062}$
2.568 ± 0.061	10^0	1.7 ± 0.3	SAL	20.7	0.082 ± 0.015
1.748 ± 0.077	10^{-2}	$7.5^{+3.8}_{-3.3}$	ANL	22.0	$0.341^{+0.173}_{-0.150}$
2.551 ± 0.077	10^0	$2.0^{+1.0}_{-0.9}$	ANL	17.8	$0.111^{+0.056}_{-0.053}$

P. Mohr and A. Matic, PRC **87**, 035801 (2013)



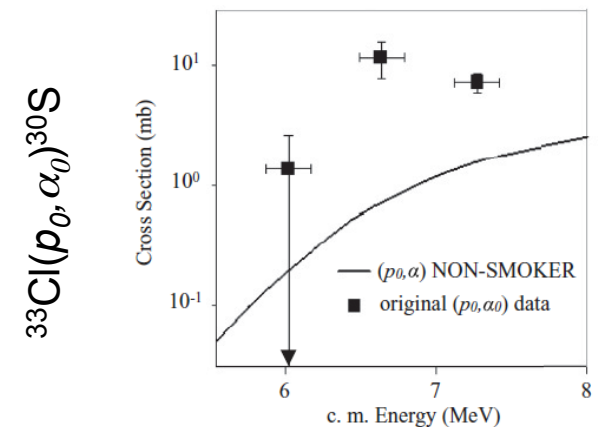
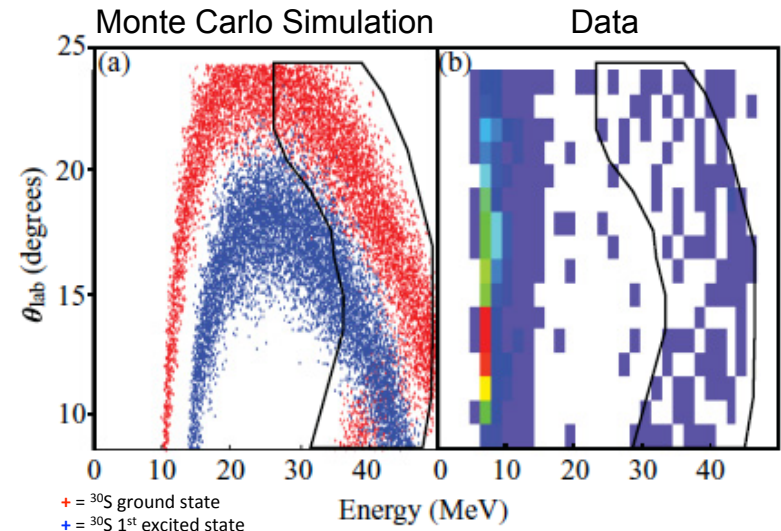
Waiting point in XRBs

- (α, p) process waiting points affect energy generation near the beginning of XRB nucleosynthesis final elemental abundances luminosity profile
- Possible (α, p) process waiting points
 - ^{22}Mg
 - ^{26}Si
 - ^{30}S
 - ^{34}Ar



Time-Inverse Studies of αp process waiting points

- Studies of the reverse time (p, α) reactions:
 - RIBs closer to stability
 - solid CH_2 targets
 - ground state \rightarrow ground state measurement only
- Studies of αp process waiting points at ATLAS
 - $^{25}\text{Al}(p, \alpha)^{22}\text{Mg}$
 - $^{29}\text{P}(p, \alpha)^{26}\text{Si}$
 - $^{33}\text{Cl}(p, \alpha)^{30}\text{S}$
 - $^{37}\text{K}(p, \alpha)^{34}\text{Ar}$



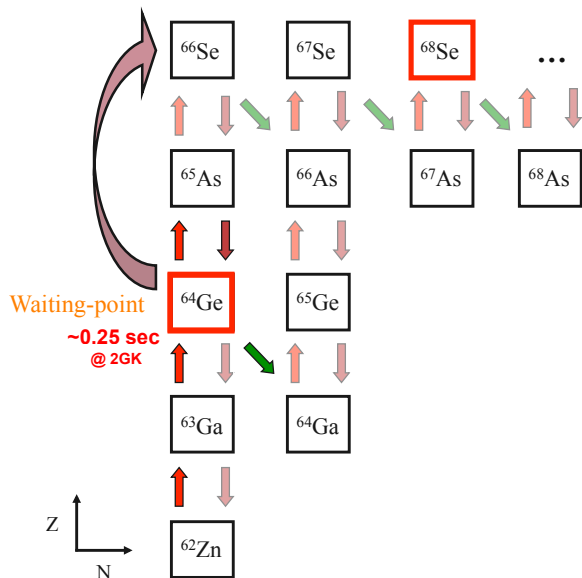
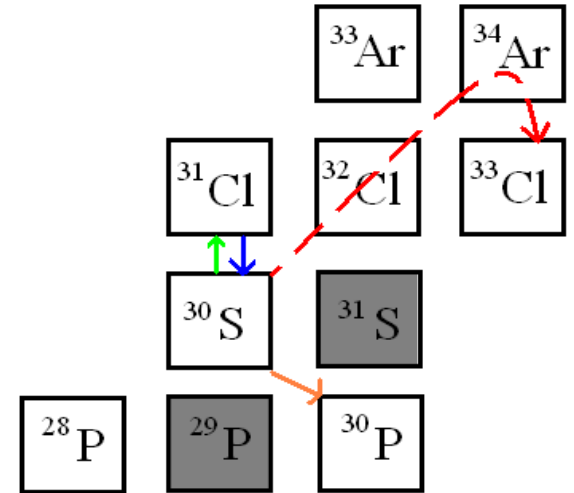
C.M. Deibel *et al*, PRC **84**, 045802 (2011).

Waiting point in XRBs

- (α, p) process waiting points affect energy generation near the beginning of XRB nucleosynthesis final elemental abundances luminosity profile

- Possible (α, p) process waiting points

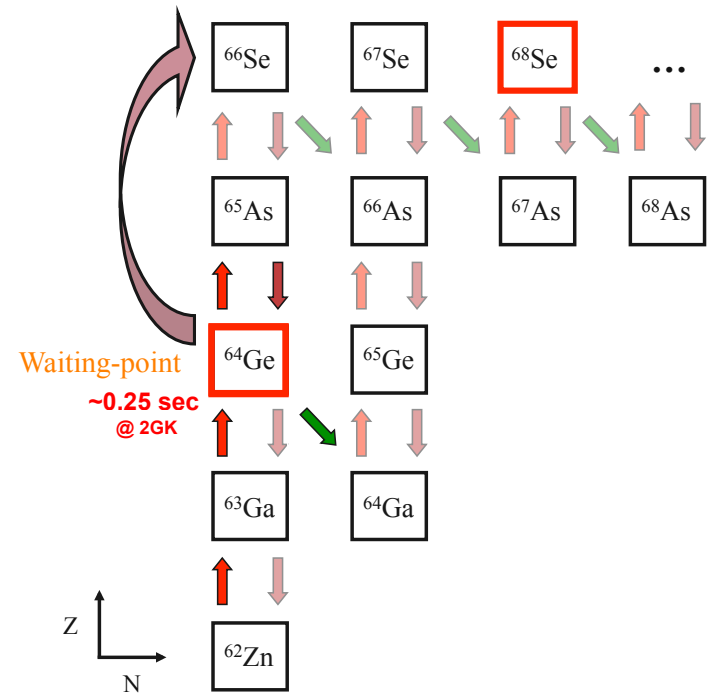
^{22}Mg
 ^{26}Si
 ^{30}S
 ^{34}Ar



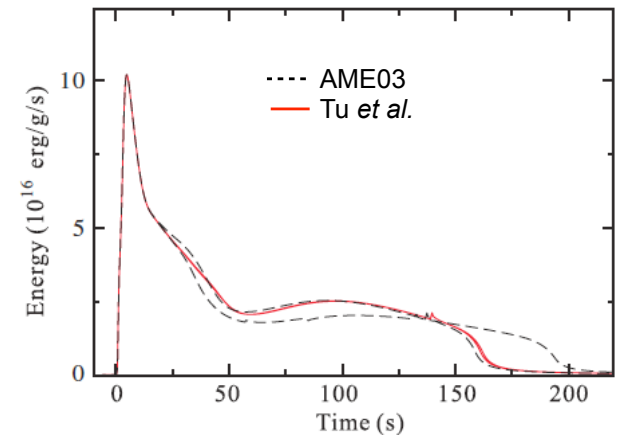
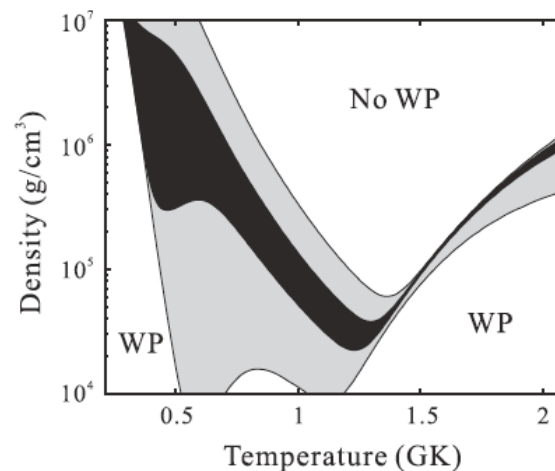
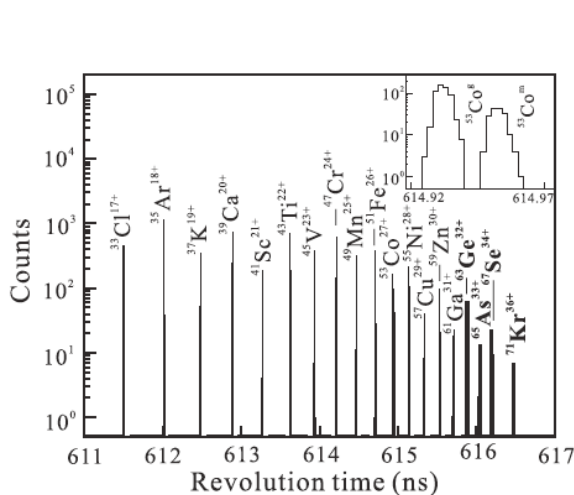
- High-mass waiting points in XRBs determine shape of light-curve tail
- Main waiting points: ^{64}Ge , ^{68}Se , ^{72}Kr
- Lifetimes well known, but not S_p 's of $Z+1$ nuclei
- ^{69}Br and ^{73}Rb both experimentally known to have negative S_p , supporting ^{68}Se and ^{72}Kr as waiting points, respectively

^{64}Ge waiting point

- Mass measurement of ^{65}As done at Lanzhou with the HIRFL-CSR (Cooler-Storage Ring)
- Projectile fragmentation of ^{78}Kr
- $S_p(^{65}\text{As}) = -90(85) \text{ keV}$: confirms ^{65}As is proton-unbound at 68.3% C.L.
- Coulomb Displacement Energy (CDE) calculations defines when ^{64}Ge is a w. p.



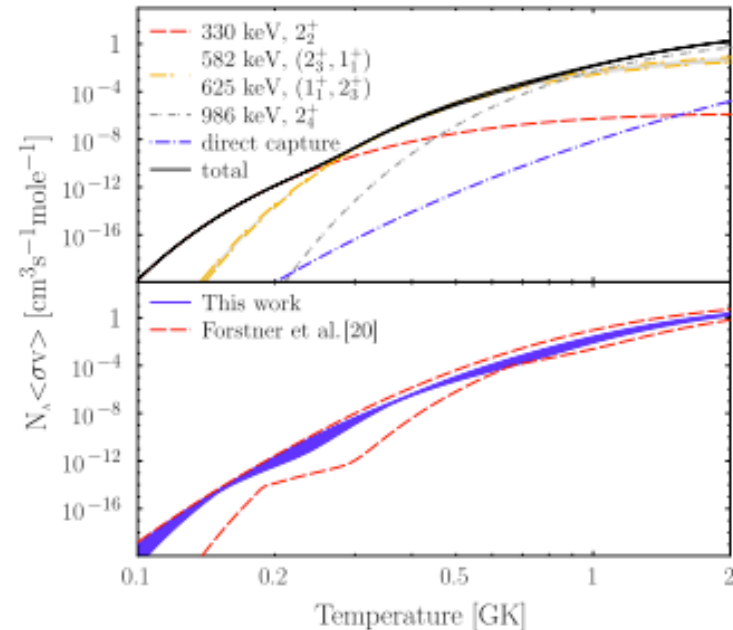
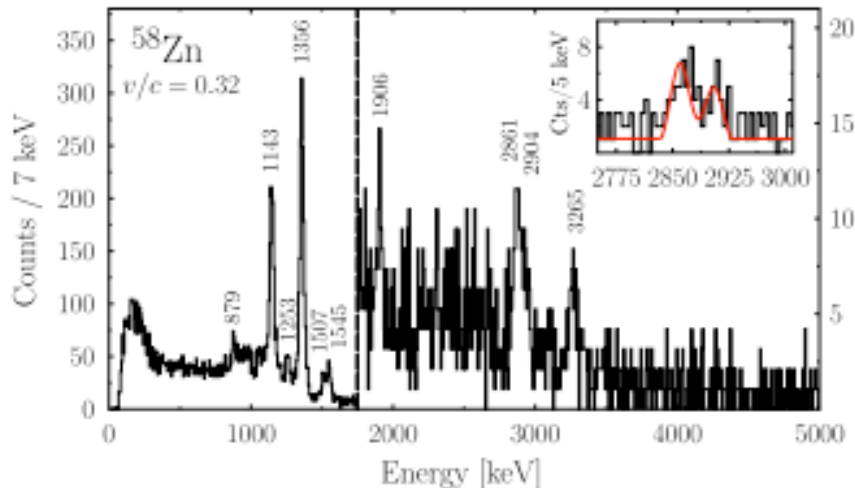
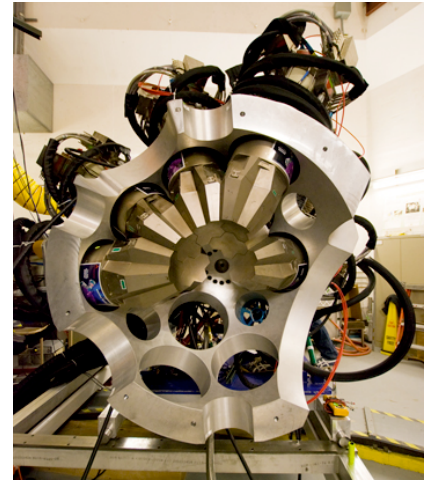
Effect of new ^{65}As mass on XRB light curve



X. L. Tu *et al.*, PRL **106**, 112501 (2011).

Indirect *rp* process measurements

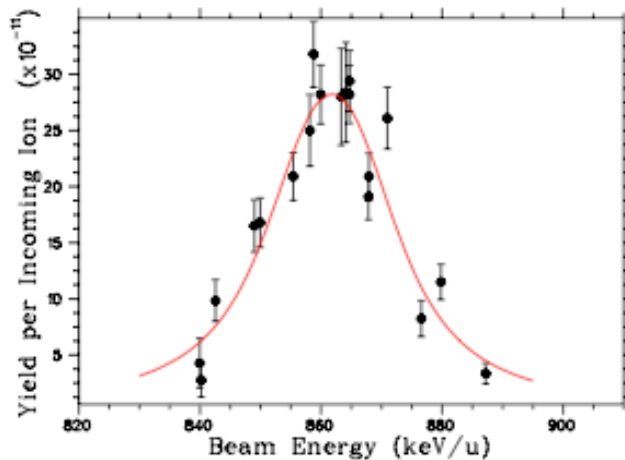
- $^{57}\text{Cu}(p,\gamma)^{58}\text{Zn}$ largest, unmeasured uncertainty in XRB nucleosynthesis around ^{56}Ni waiting point
- Studied $d(^{57}\text{Cu}, ^{58}\text{Zn})n$ at NSCL
 - ^{58}Zn identified with S800
 - γ rays from $^{57}\text{Cu}^*$ detected with GRETINA
- Measurements of resonance energies and tentative spins reduce reaction rate uncertainties by 3 orders of magnitude



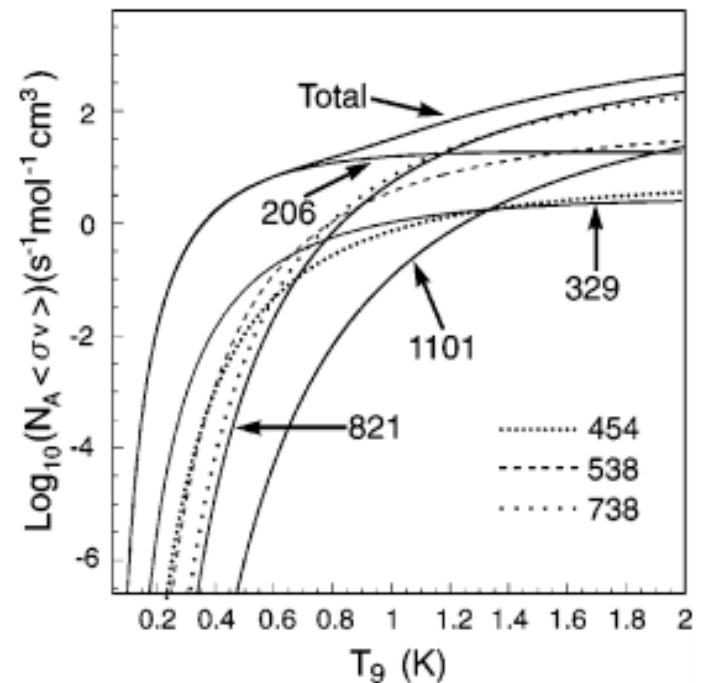
C. Langer *et al.*, PRL **113**, 032502 (2014)

Direct rp process measurements

- $^{21}\text{Na}(p,\gamma)^{22}\text{Mg}$ direct measurement with DRAGON at TRIUMF
 - ^{21}Na ISOL produced beam
 - extended H_2 target
 - coincidence measurement
- Inclusion of directly measured rate shows small differences in XRB peak timing and total luminosity



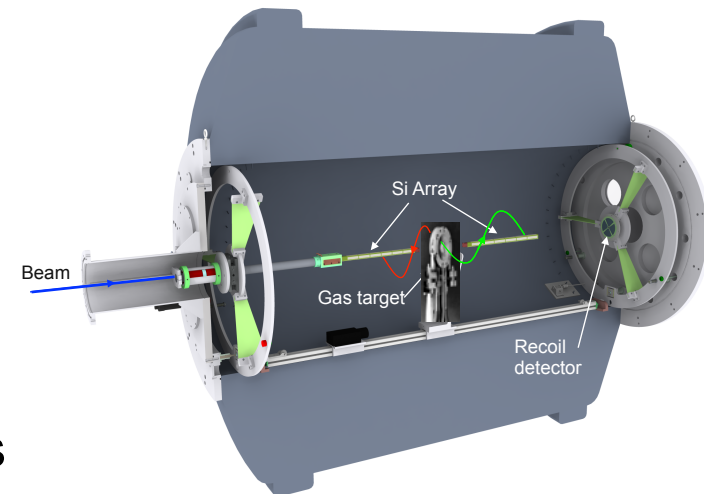
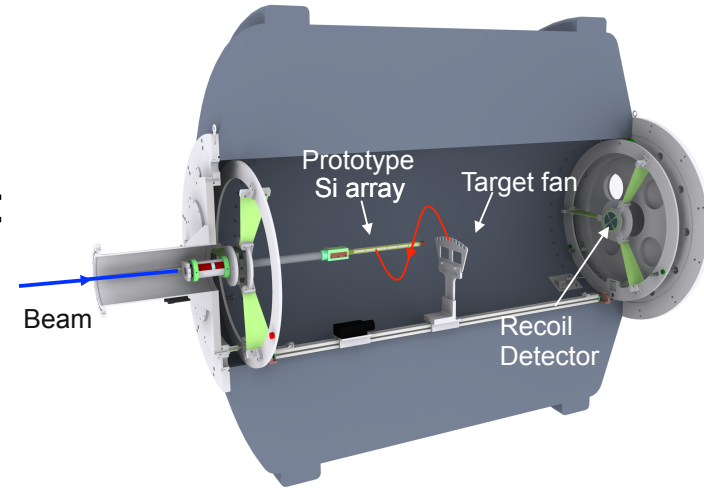
A. A. Chen *et al.*, NPA **A752**, 510 (2005)



J. M. D'Auria *et al.*, PRC **69**, 065803 (2004).

Future: Direct (α, p) Studies with HELIOS

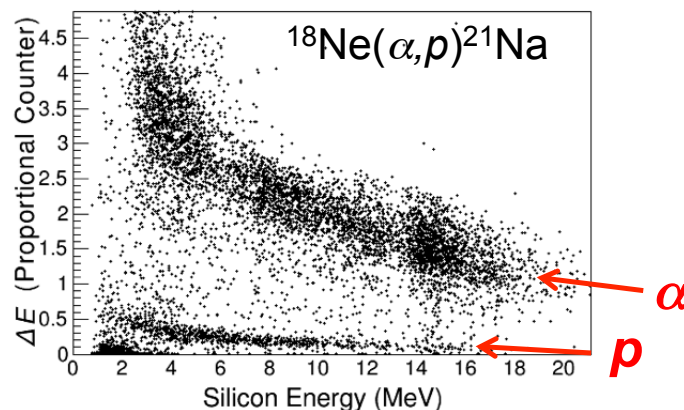
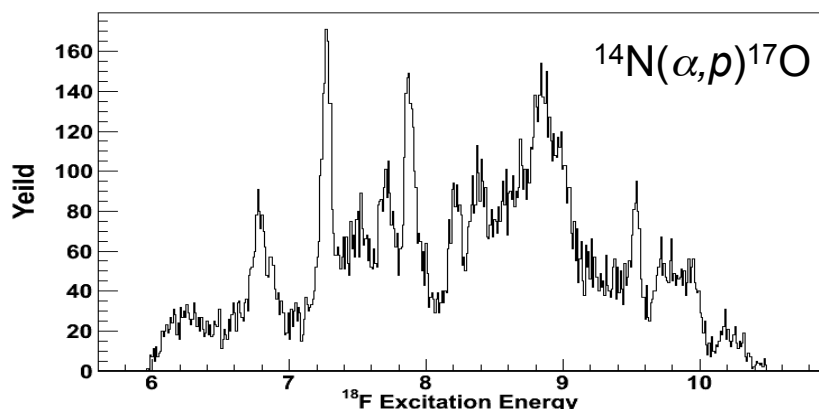
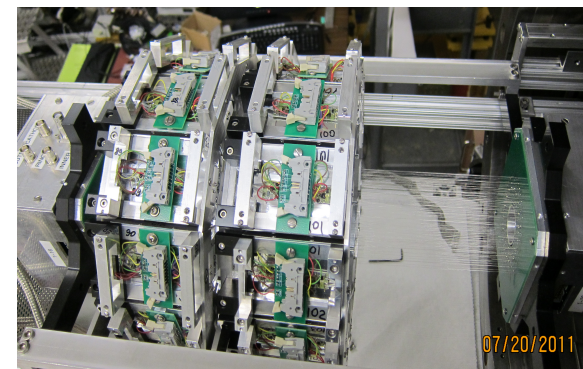
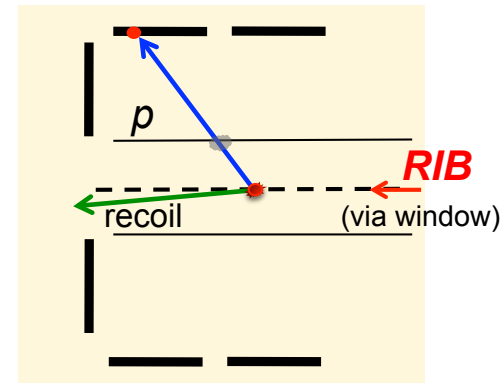
- HELical Orbit Spectrometer (HELIOS)
 - 2.85 T repurposed MRI magnet
 - allows improved inverse kinematics studies:
 - high geometrical efficiency
 - better resolution (alleviates kinematic compression)
 - unique particle ID via time-of-flight
- Upgrades to HELIOS for (α, p) studies:
 - cryogenic gas target
 - commissioned Spring 2013
 - high-rate ionization chamber
 - commissioned Spring 2013
 - new Si array
 - under construction
- Beam development underway at ANL
 - AIRIS upgrade for future high intensity RIBs





Current Developments: ANASEN

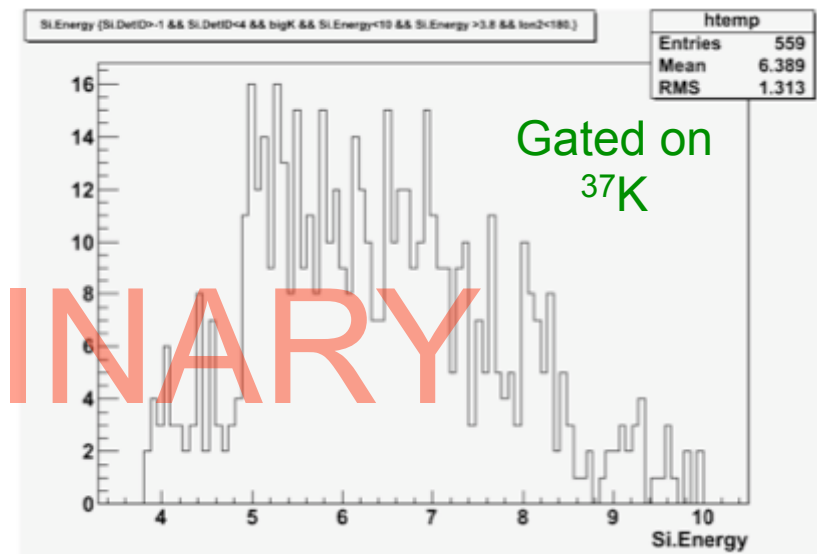
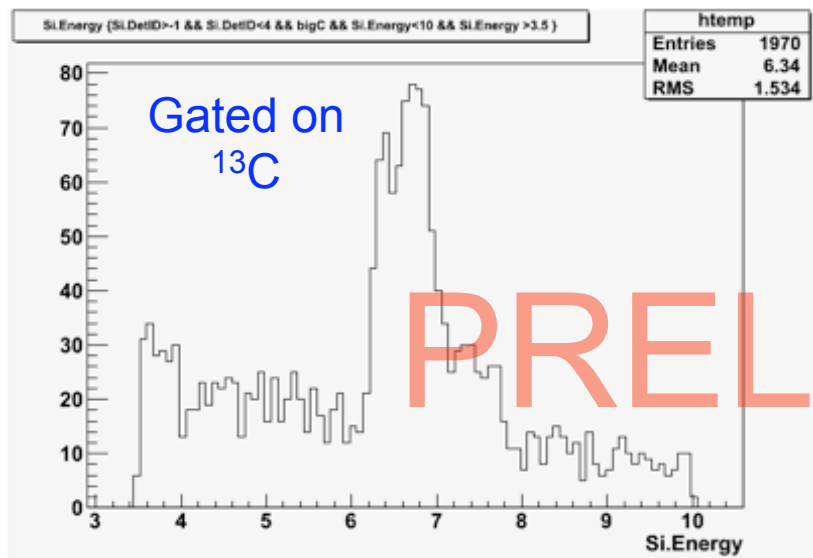
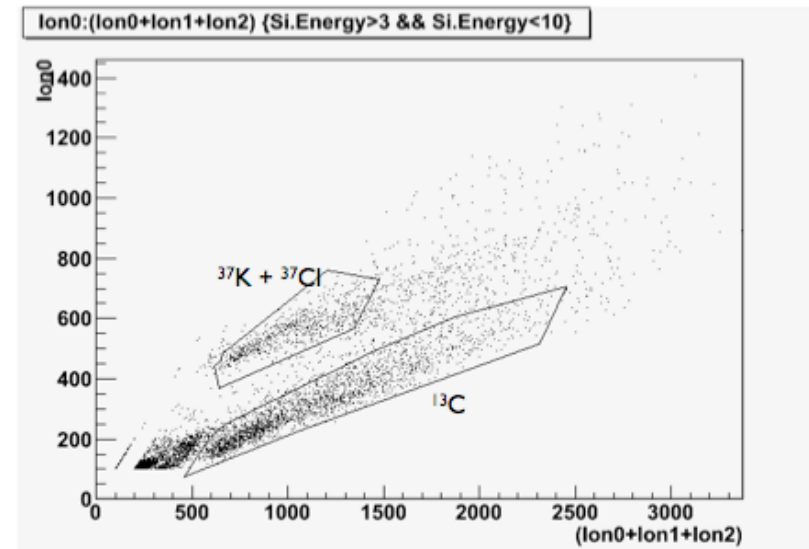
- Array for Nuclear Astrophysics and Structure with Exotic Nuclei
 - designed for direct (α, p) reaction studies
 - extended, active gas target
 - proportional counter
 - Si detector array
- Nuclear Astrophysics measurements:
 - $^{14}\text{N}(\alpha, p)^{17}\text{O}$ (stable beam FSU)
 - $^{18}\text{Ne}(\alpha, p)^{21}\text{Na}$ (RIB from RESOLUT @ FSU)
 - $^{37}\text{K}(p, p)^{37}\text{K}$ (first RIB measurement @ ReA3)



ANASEN at ReA3:

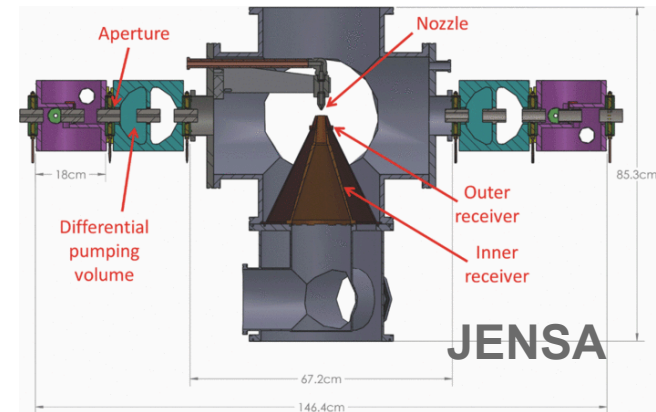
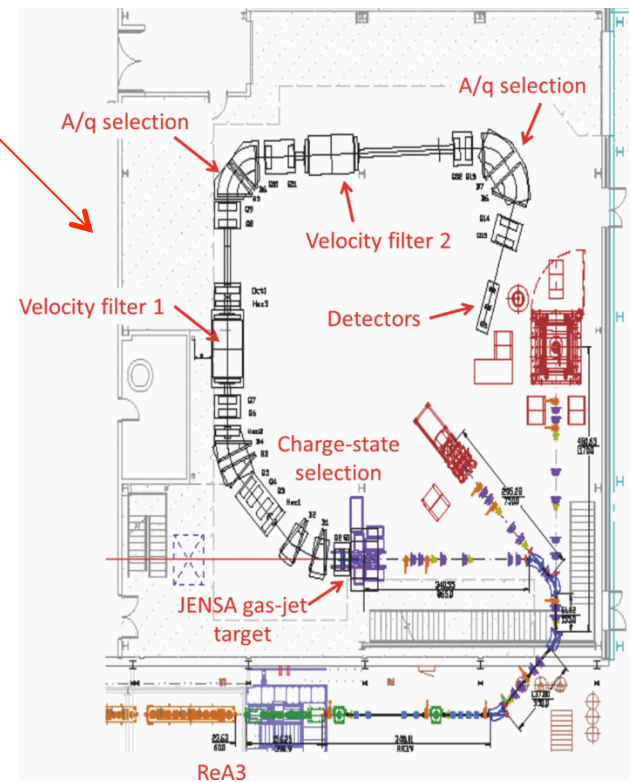
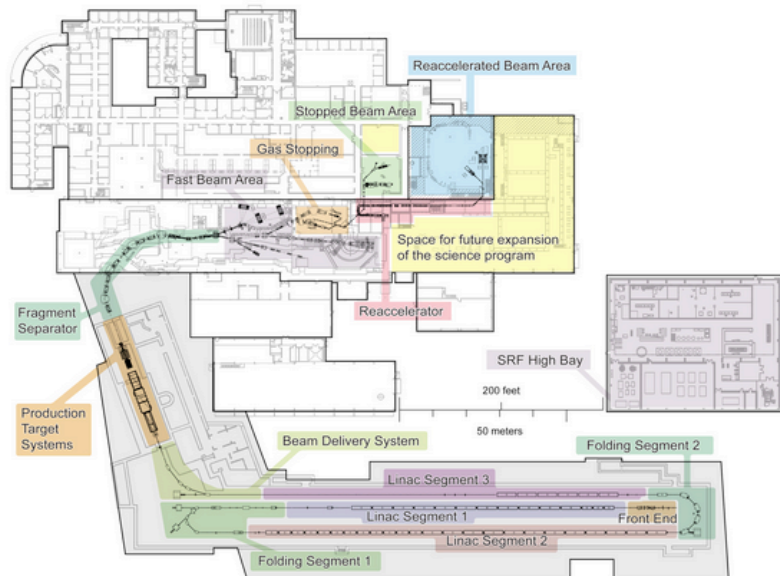


- First measurement with reaccelerated beams at ReA3 @ Michigan State University:
 - reaccelerated ^{37}K beam
 - CH_2 target
- Coincidence measurement
 - scattered protons detected in ANASEN Si array
 - Heavy recoils detected in ionization chamber



Future Direct Studies: SECAR

- Recoil separator planned for ReA/FRIB at Michigan State University
- Targets:
 - windowless gas target JENSA already installed at ReA
 - extended gas target to be developed
- Direct measurements of (p, γ) and (α, γ) reactions
 - capture on nuclei up to $A = 65$
 - 1×10^{-17} rejection



S. D. Pain, AIP 4, 041015 (2014)

Summary

- Most work on XRB reaction rates consists of indirect measurements:
 - transfer reactions with stable beams
 - time-inverse reaction studies with RIBs
- Needs for direct reaction measurements:
 - high-intensity, low energy radioactive beams
 - high density gas targets
 - recoil separators
 - other novel experimental techniques (e.g. active gas targets)
- Other needs:
 - *rp* process mass measurements
 - indirect measurements of relevant nuclear structure information
 - specific observations data (e.g. isotopic measurements)
 - more realistic modeling

Thank you!